

University of Groningen

Analysis of the structure and substrate scope of chitooligosaccharide oxidase reveals high affinity for C2-modified glucosamines

Savino, Simone; Jensen, Sonja; Terwisscha van Scheltinga, Anke; Fraaije, Marco W

Published in:
FEBS Letters

DOI:
[10.1002/1873-3468.13854](https://doi.org/10.1002/1873-3468.13854)

IMPORTANT NOTE: You are advised to consult the publisher's version (publisher's PDF) if you wish to cite from it. Please check the document version below.

Document Version
Version created as part of publication process; publisher's layout; not normally made publicly available

Publication date:
2020

[Link to publication in University of Groningen/UMCG research database](#)

Citation for published version (APA):

Savino, S., Jensen, S., Terwisscha van Scheltinga, A., & Fraaije, M. W. (2020). Analysis of the structure and substrate scope of chitooligosaccharide oxidase reveals high affinity for C2-modified glucosamines. *FEBS Letters*, 594(17), 2819-2828. <https://doi.org/10.1002/1873-3468.13854>

Copyright

Other than for strictly personal use, it is not permitted to download or to forward/distribute the text or part of it without the consent of the author(s) and/or copyright holder(s), unless the work is under an open content license (like Creative Commons).

Take-down policy

If you believe that this document breaches copyright please contact us providing details, and we will remove access to the work immediately and investigate your claim.

Downloaded from the University of Groningen/UMCG research database (Pure): <http://www.rug.nl/research/portal>. For technical reasons the number of authors shown on this cover page is limited to 10 maximum.



DR. SIMONE SAVINO (Orcid ID : 0000-0001-9505-3348)

DR. MARCO FRAAIJE (Orcid ID : 0000-0001-6346-5014)

Received Date : 01-May-2020

Revised Date : 27-May-2020

Accepted Date : 27-May-2020

Article type : Research Articles

Analysis of the structure and substrate scope of chitooligosaccharide oxidase reveals high affinity for C2-modified glucosamines

Simone Savino^a, Sonja Jensen^a, Anke Terwisscha van Scheltinga^a, Marco W. Fraaije^{a*}

Simone Savino: ORCID ID 0000-0001-9505-3348

Sonja Jensen: ORCID ID 0000-0003-1372-2275

Marco Fraaije: ORCID ID 0000-0001-6346-5014

^a Molecular Enzymology Group, University of Groningen, Nijenborgh 4, 9747AG Groningen, The Netherlands; *Correspondence to: m.w.fraaije@rug.nl

Abstract

Chitooligosaccharide oxidase (ChitO) is a fungal carbohydrate oxidase containing a bicovalently bound FAD cofactor. The enzyme is known to catalyse the oxidation of chitooligosaccharides, oligomers of N-acetylated glucosamines derived from chitin degradation. In this study, the unique substrate acceptance was explored by testing a range of N-acetyl-D-glucosamine derivatives, revealing that ChitO preferentially accepts carbohydrates with a hydrophobic group attached to C2. The enzyme also accepts streptozotocin, a natural product used to treat tumours. Elucidation of the crystal structure provides an explanation for the high affinity towards C2-decorated glucosamines: the active site has a secondary binding pocket that accommodates groups attached

This article has been accepted for publication and undergone full peer review but has not been through the copyediting, typesetting, pagination and proofreading process, which may lead to differences between this version and the [Version of Record](#). Please cite this article as [doi: 10.1002/1873-3468.13854](https://doi.org/10.1002/1873-3468.13854)

This article is protected by copyright. All rights reserved

at C2. Docking simulations are fully in line with the observed substrate preference. This work expands the knowledge on this versatile enzyme.

Keywords: Covalent flavin, glucosamine, oxidation, crystal structure, chitooligosaccharides

Abbreviations: ChitO, chitooligosaccharide oxidase; GOO, glucooligosaccharide oxidase; GlcNAc, N-acetyl-D-glucosamine; GlcVal, N-valeryl-D-glucosamine; GlcPro, N-propionyl-D-glucosamine; GlcHex, N-hexanoyl-D-glucosamine; FAD, flavin adenine dinucleotide; CV, column volume; MBP, maltose binding protein; HRP, horseradish peroxidase; RMSD, root mean square deviation; SEC, size exclusion chromatography.

Highlights

- The crystal structure of ChitO was solved for the first time
- The substrate range of ChitO was further expanded towards C2-glucosamines
- Docking experiments explained the substrate acceptance of ChitO

Introduction

Carbohydrate oxidases are highly valued enzymes, used in diagnostics and for industrial applications because of their enantio- and regioselectivity [1]. They are active on various carbohydrates and are typically regioselective in oxidizing a particular CH-OH bond of the targeted carbohydrate. Upon oxidation of the carbohydrate, molecular oxygen is reduced into hydrogen peroxide. Often, alternative electron acceptors can be used as well, such as quinones or ferrocenium ion [2]. Two distinct groups of carbohydrate oxidases can be distinguished: copper- and FAD-containing oxidases. Oxidases of the first group are mostly active on monosaccharides such as galactose [3]. They display sequence and structural features which distinguish them from FAD-dependent oxidases, such as clusters of histidine residues to coordinate copper [4]. The FAD-containing oxidases can be classified based on different parameters such as their substrate specificity, mode of flavin cofactor binding or structural features. The most studied and widely applied carbohydrate oxidase is glucose oxidase from *Aspergillus niger* [5]. It contains a dissociable but tightly bound FAD as cofactor and is active on monosaccharides with a preference for D-glucose, performing oxidation at the C1 of the sugar ring. The active site is partially occluded, leaving space for a single sugar moiety to enter through a narrow tunnel which opens in a funnel on the protein surface. Glucose oxidase is a prototypical member of the GMC

flavoprotein family [6]. Another GMC-type flavoprotein carbohydrate oxidase is pyranose oxidase [7, 8], in which the FAD is covalently tethered via a histidyl linkage between His167 and the C8 of the isoalloxazine ring of the flavin cofactor. The oxidation reaction in this case involves an oxidation at the C2 position of various pyranoses, such as D-glucose. Similar to glucose oxidase, pyranose oxidase has a buried active site that can be reached through a narrow substrate tunnel.

A completely different fold is adopted by flavoprotein carbohydrate oxidases that contain a bicovalently bound FAD. They are part of the VAO flavoprotein family [9] and are set apart from all above-mentioned carbohydrate oxidases because of their activity on oligosaccharides [10]. This atypical anchoring of the FAD cofactor involves a histidyl and a cysteinyl linkage. While the presence of one covalent flavin-protein linkage has been linked to enhanced stability and redox potential [11, 12], the presence of two covalent bonds has been hypothesized to enhance capacity of these enzymes to bind and oxidise relatively large substrates such as oligosaccharides. Through the two attachment points, the flavin cofactor is fixed and the surrounding protein part can adopt a relatively open active site as observed for the crystal structures of bicovalent flavoproteins.

Glucooligosaccharide oxidase (GOO) was the first bicovalent flavoprotein for which the crystal structure was elucidated [13, 14]. GOO performs oxidation at the C1 of aldose sugar molecules. GOO is efficient in oxidizing disaccharides such as lactose, maltose and cellobiose, but is even more active on xylooligosaccharides, as demonstrated by recent studies [15, 16]. It performs oxidation at C1 which means that, for oligosaccharides, the target of the reaction is exclusively the CH-OH bond at the reducing end of the polymer chain. The structure of GOO revealed for the first time the structural architecture of a bicovalently bound FAD cofactor, linked to the enzyme via histidyl and cysteinyl linkage [13]. Even though the two linking residues are 60 positions apart in the amino acid sequence, the two covalent bonds are structurally close. The histidyl linkage is formed with C8 of the isoalloxazine ring while C6 is engaged in the cysteinyl linkage. By site-directed mutagenesis studies it has been shown that both covalent bonds contribute to a relatively high redox potential of the flavin cofactor and are required for proper catalysis [14]. The reaction mechanism of GOO involves a strategically positioned tyrosine residue behaving as a general base, acting in concert with the flavin to catalyse oxidation via a hydride transfer.

In addition to GOO, several other sequence- and structure-related carbohydrate oxidases have been discovered in the last two decades [15, 16]. While some of them exhibit a similar substrate acceptance profile and regioselectivity, several were found to act on other types of carbohydrates. We have recently reported on a xylooligosaccharide oxidase from *Myceliophthora thermophila*

which specifically acts on xylose-based oligosaccharides, while oxidizing at C1 [17]. The elucidated crystal structure revealed the structural features that result in this unique substrate specificity. Another example of a carbohydrate oxidase belonging to this group of bicovalent flavoprotein oxidases, that displays activity on a different class of carbohydrates, is chitooligosaccharide oxidase from the fungus *Fusarium graminearum*. Chitooligosaccharides can be derived from chitin and have found industrial applications [18]. Similar to GOO, ChitO catalyses oxidation at C1, while it displays a unique substrate specificity: it acts on N-acetylated oligosaccharides, namely chitooligosaccharides (Fig. 1) [19]. This means that ChitO can recognise oligomers of N-acetylglucosamine, bind them and position their reducing end towards its active site to catalyse the oxidation reaction at C1. The specificity towards N-acetylated carbohydrates has been previously ascribed to a pivotal role of a glutamine residue (Gln268) in the substrate binding pocket [19]. Yet, no crystal structure was available to confirm this role. Mutagenesis studies have confirmed that it harbours a bicovalently bound FAD, attached to cysteine and histidine residues, as in the case of GOO. The impairment of a formation of the covalent bonds strongly reduces the redox potential of ChitO [20].

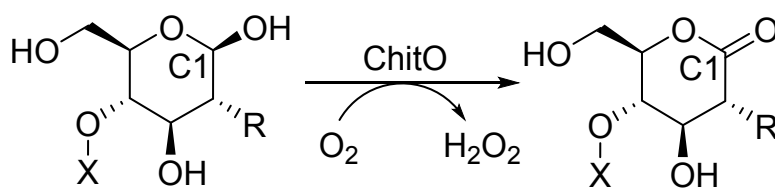


Fig. 1: General reaction catalysed by ChitO.

$X=H$ for monomers or other N-acetylglucosamine moieties for oligomers. R = variable substituent.

Using a homology model of ChitO, an enzyme engineering study has been carried out which resulted in enzyme variants that accept substrates other than N-acetylated oligosaccharides [21]. In this way it was possible to expand the activity of ChitO towards the disaccharide lactose and the monosaccharide N-acetyl-D-glucosamine. It was also demonstrated that ChitO and its variants can be used for a convenient assay for monitoring hydrolysis of chitin or cellulose [22].

Here, we report on the crystal structure of ChitO. Furthermore, using the obtained structural insights, we have performed a more exhaustive study on the substrate scope of ChitO. Various amino sugars have been tested as substrates, to better understand the substrate acceptance profile

of ChitO. Intriguingly, this has revealed that this fungal oxidase readily accepts various aliphatic groups at C2 of glucooligosaccharides. These findings add more insight into the catalytic scope of ChitO and its structural features.

Materials and methods

The reagents used in this study were from Sigma, Acros and BioRad, culture media components were from Difco and the crystallisation screens were purchased from Hampton, Molecular Dimensions and Qiagen.

Protein expression and purification – chemically competent ORIGAMI *E. coli* cells were transformed using the plasmid harbouring the gene for expression of MBP-ChitO [19]. After growth on LB-agar containing ampicillin, tetracycline and kanamycin, colonies were picked and used for inoculation of small scale cultures of LB medium. After overnight growth at 37°C, the precultures were used to inoculate Erlenmeyer flasks. The LB medium was complemented with 0.04% L-arabinose to induce protein expression and the flasks were left incubating at 17°C for 3 days at 200 rpm. After harvesting by centrifugation, the cell pellet was resuspended in buffer A (50 mM KPi buffer pH 7.6) and the suspension sonicated for 10 minutes (5 seconds on – 5 seconds off) at 70% amplitude on a Vibra Cell CV 18 sonicator (Sonic). The lysate underwent ultracentrifugation and the supernatant was collected and filtered using 0.4 µm filter units (Millipore).

Gravity columns were filled with amylose resin and rinsed with 5 CV of buffer A. After loading of the sample on the column, elution was performed with 3 CV of buffer A followed by elution with 2 CV of buffer B (50 mM KPi pH 7.6 and 10 mM maltose). Cleavage of MBP was performed in batch using 0.6 µg of trypsin per mg of protein content, at room temperature for 1.5 hours. ChitO was separated from the cleaved MBP by loading the sample on the amylose resin column and by collecting the flow-through (Fig. S1).

Size exclusion chromatography and buffer exchange were necessary for crystallisation experiments on ChitO, to assure monodispersity and to minimise salt crystals growth, respectively. A Superdex 200 10/300 column (GE Healthcare) was mounted on an ÄKTA purifier (GE Healthcare) and equilibrated in a buffer containing 20 mM Na-citrate pH 4 and 100 mM NaCl. Protein was injected and the system flow set to 0.2 mL/minute. Fractions of 0.5 mL were collected and the ones corresponding to the yellow-coloured ChitO elution peak were pooled and concentrated (Figs. S2 and S3).

Kinetic studies – An HRP coupled assay was used to detect ChitO activity [19] in microtiter plates using a SynergyMX (BioTek) plate reader. Measurements of absorbance increase at a wavelength of 515 nm were performed over a period of 15 minutes from the start of the reaction. The tested substrates for these studies were GlcNAc, streptozotocin, GlcPro, GlcVal and GlcHex.

Melting temperature assay – ChitO samples were tested for their thermostability using different buffers employing both the ThermoFluor and ThermoFAD [23] methods. In the first case SYPRO orange dye was added in order to detect protein denaturation, while in the second method the fluorescent signal of the flavin cofactor was used. The measurements were performed using an ICycler MyiQ thermocycler (BioRad), applying a temperature rampage from 23 to 100°C and recording the fluorescence signal every 0.5 minutes. The tested pH values of the buffers in which ChitO was dissolved ranged from 3 to 8.5, with concentrations of 100 mM.

Protein crystallisation and crystallography – ChitO crystals were obtained in multiple conditions. Crystallisation conditions were screened using a Mosquito crystallisation robot (TPP LabTech). After careful optimisation, the best diffracting objects were determined to be in a handmade sitting drop condition containing 0.3 M CaCl₂, 0.1 M Bis-Tris pH 5.7 and 34% w/v PEG 3350. Due to their intergrown state, these crystals were separated using microtools. After treatment with a glycerol-based cryoprotectant and freezing in liquid nitrogen, the samples were sent for synchrotron data collection (Table 1).

Table 1: Data collection and refinement statistics.

Statistics for the high-resolution shell are shown in parenthesis.

| | |
|--------------------|-------------------------------|
| Resolution range | 36.84 - 1.611 (1.668 - 1.611) |
| Space group | P 21 21 21 |
| Unit cell | 73.686 74.247 97.157 90 90 90 |
| Total reflections | 133786 (10473) |
| Unique reflections | 67364 (5457) |
| Multiplicity | 2.0 (1.9) |
| Completeness (%) | 96.84 (79.79) |
| Mean I/sigma(I) | 20.59 (2.00) |
| Wilson B-factor | 21.47 |
| R-merge | 0.01763 (0.3768) |
| R-meas | 0.02493 (0.5328) |

| | |
|--------------------------------|------------------|
| R-pim | 0.01763 (0.3768) |
| CC1/2 | 1 (0.698) |
| CC* | 1 (0.907) |
| Reflections used in refinement | 67361 (5457) |
| Reflections used for R-free | 3242 (278) |
| R-work | 0.1780 (0.2592) |
| R-free | 0.1989 (0.2498) |
| CC(work) | 0.964 (0.788) |
| CC(free) | 0.958 (0.816) |
| Number of non-hydrogen atoms | 3934 |
| macromolecules | 3527 |
| ligands | 53 |
| solvent | 354 |
| Protein residues | 468 |
| RMS(bonds) | 0.016 |
| RMS(angles) | 1.92 |
| Ramachandran favoured (%) | 98.28 |
| Ramachandran allowed (%) | 1.5 |
| Ramachandran outliers (%) | 0.21 |
| Rotamer outliers (%) | 0.27 |
| Clashscore | 8.94 |
| Average B-factor | 24.6 |
| macromolecules | 23.98 |
| ligands | 16.81 |
| solvent | 32.03 |

The diffraction data on ChitO crystals were collected at the SLS, Villigen, Switzerland, where one object diffracted at 1.6 Å resolution. The collected images were processed using *XDS* [24] and the resulting *ASCII* file was used for scaling in *aimless* from the CCP4 package [25]. The scaled *.mtz* file obtained from *aimless* was the input for the structure solution step run in *phaser MR* [26]. The search model for molecular replacement was the PDB entry 1ZR6, having 45% identity with

ChitO over 94% query cover (from BlastP run). Six cycles of *refmac5* [25] and manual fitting in *coot* [27] delivered the final model.

Docking and modelling studies – The high resolution structure of ChitO was further analysed by docking known substrates in the active site of the enzyme. For this procedure *Yasara* [28] docking was used, applying the *AmberIPQ* force field over a 20x20x20Å box, which was encompassing the whole active site. The enzyme structure and the structures of the different ligands were provided as *.pdb* files and the docking experiments were launched for 100 runs using *VINA* [29]. The results were clustered in values of RMSD which were changed each time to allow a consistent number of representative complexes to be inspected visually. The complexes giving a pro-catalytic arrangement, underwent an energy minimisation step in *Yasara*. This procedure was adopted for the ligands: GlcNAc, streptozotocin, chitobiose, GlcVal, chitotriose, cellobiose, maltose and lactose. When the dockings of GlcHex and N-octyl-D-glucosamine (GlcOct) were tested, a more accurate protocol was followed, due to the bulky nature of the compounds. In these instances, some of the residues forming the binding pocket were allowed to move during the docking experiment (Thr153, Met170 and Phe319). The *.pdb* file of the ChitO structure was prepared by running *Protoss* on Protein Plus [30] and then by creating a rigid and a flexible sets of coordinates for the receptor and a flexible set for the ligand using *AutoDock Tools*. The structures were converted in *.pdbqt* format to ensure proper charges and connectivity and a config file was written to run *VINA* over a defined 20x20x20Å box which was traced in *Pymol* [34] and then imported. After converting the resulting models in *.pdb* files and selecting the results that showed a proper conformation, these underwent an energy minimisation step in *Yasara*.

Results and discussion

ChitO is a VAO-type enzyme displaying high sequence homology with other known oligosaccharide oxidases. It also has a bicovalently bound FAD cofactor present in its active site, like many other VAO-type oxidases active on oligosaccharides. The main trait distinguishing ChitO from other flavoprotein oxidases active on oligosaccharides is the substrate specificity. While GOO and XylO display specificity for glucooligosaccharides and xylooligosaccharides, respectively, ChitO shows a high affinity for oligosaccharides that are N-acetylated at C2 (N-acetylglucooligosaccharides). In the present study, wild type ChitO was purified and crystallised, and its kinetic profile determined for a set of D-glucosamine derivatives.

The main goal of our study was to determine the molecular basis for the unique substrate acceptance of ChitO. In order to investigate what type of C2-modified saccharides are still accepted as substrate, potential substrates with different C2-moieties were systematically screened. Next to the previously identified substrate N-acetylglucosamine (GlcNAc), also other compounds were tested with the alkyl tail extended by one carbon (N-propionyl-D-glucosamine, GlcPro), three carbons (N-valeryl-D-glucosamine, GlcVal), and four carbons (N-hexanoyl-D-glucosamine, GlcHex). Additionally, a nitrosourea derivative of D-glucosamine was tested: streptozotocin (Fig. 2). Streptozotocin is a natural product and has been shown to be a valuable high-toxicity anti-cancer agent which damages DNA [35]. Intriguingly, all test D-glucosamine derivatives were found to be accepted as substrate. After establishing the steady-state kinetic parameters (Table 2 and Fig. S4), it was found that streptozotocin is the worst substrate out of the five tested. Yet, its kinetic parameters are not much different from D-glucosamine. When considering the kinetic parameters, the best identified substrate is GlcHex. The catalytic efficiency for this monosaccharide is even superior to any previous reported ChitO substrate [22]. The differences in catalytic efficiency rely mainly on the varying K_m values while the k_{cat} is rather similar for all substrates. With GlcHex displaying a K_m of only 0.16 mM, the apparent affinity steadily decreases going to shorter alkyl moieties at C2. This behaviour suggested the presence of structural elements capable of favourable hydrophobic interactions with the moiety present at C2 (Table 2 and Fig. S4).

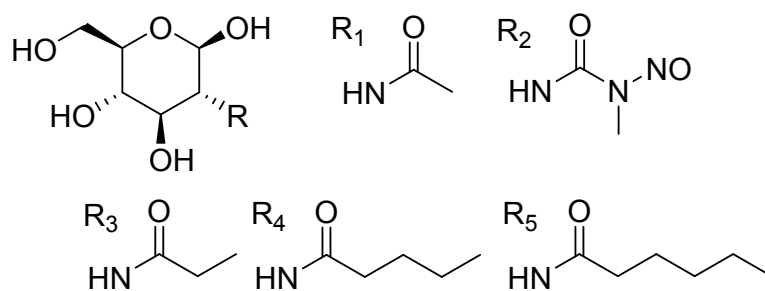


Fig. 2: Structural formulas of the tested substrates.

R_1 is GlcNAc, R_2 is streptozotocin, R_3 is GlcPro, R_4 is GlcVal and R_5 is GlcHex.

Table 2: Steady-state kinetic parameters for the identified ChitO substrates.

| | K_m (mM) | k_{cat} (s^{-1}) | k_{cat}/K_m ($M^{-1} s^{-1}$) |
|-----------------------|-----------------|------------------------|-----------------------------------|
| Streptozotocin | 6.24 ± 0.47 | 7.14 ± 0.15 | 1140 |
| GlcNAc | 5.10 ± 0.47 | 9.02 ± 0.30 | 1770 |

| | | | |
|---------------|-------------|-------------|-------|
| GlcPro | 0.94 ± 0.03 | 7.88 ± 0.09 | 8350 |
| GlcVal | 0.35 ± 0.01 | 8.30 ± 0.05 | 23600 |
| GlcHex | 0.16 ± 0.01 | 9.45 ± 0.09 | 59100 |

To establish optimal handling conditions for ChitO, the thermostability was probed. The apparent melting temperature (T_m) of ChitO was assessed in different buffer conditions using two methods: ThermoFAD and ThermoFluor. Despite ChitO being a flavoenzyme, ThermoFAD measurements did not give proper melting curves. This is probably occurring because the flavin cofactor is covalent tethered which results in fluorescence quenching, even upon unfolding of the protein. ThermoFluor resulted in clear unfolding events and was used over a range of pH values (pH 3 – 8.5) and NaCl concentrations (0.02 - 0.50 M). The highest T_m measured for ChitO was 63.0°C, which was measured in Na-citrate buffer pH 4.0 (Fig. S5). Based on these results, the mentioned buffer, provided with additional 0.02 M NaCl, was used to run size exclusion chromatography, with the aim of stabilising the target protein as much as possible before crystallisation experiments. This led to successful crystallization of the oxidase.

The crystal structure of ChitO (PDB entry 6Y0R) was refined at 1.6 Å resolution. The space group is $P2_12_12_1$ and the unit cell parameters are $a=73.69$ $b=74.25$ $c=97.16$, consistent with the monomeric arrangement of the crystal structure for a 50 kDa protein, and with the calculated Matthews coefficient of 2.66, corresponding to 53.78% of solvent content. The crystallographic parameters are listed in Table 1. The crystal structure of ChitO corresponds to a monomer of 467 traced residues. This is also the oligomeric state of the protein as determined by gel permeation chromatography (Fig. S2). One disulfide bond is present, which keeps the N-terminus close to the protein core by linking Cys6 and Cys79. This also explains why expression of ChitO required *E. coli* ORIGAMI which promotes disulfide bond formation [12]. Different from the elucidated GOO structures, no glycosylation was found on surface residues. This reflects the fact that ChitO was recombinantly produced using *E. coli*. Some residues, such as Asn327, may represent glycosylation sites, being exposed on the surface and overlapping with corresponding glycosylated residues present in GOO. One FAD cofactor per protomer is bound in the active site, at the interface between the FAD-binding (F) and substrate-binding (S) domains (Fig. 3). The F domain can be roughly described as the N-terminal portion of the protein, until residue 230 complemented with residue 440 to the C terminus (Fig. 3). The S domain corresponds to the central part of the sequence, from residue 231 to residue 439. While no substrate is bound in the elucidated structure

of ChitO, the location of the carbohydrate binding pocket along the isoalloxazine moiety of the FAD cofactor can be easily identified by overlapping the structure with a GOO or XylO structure. In fact, superposition of ChitO with GOO and XylO reveals a high structural similarity, with RMSD of only 1.08 Å when comparing to GOO (PDB entry 2AXR) and 1.13 Å when comparing to XylO (PDB entry 5L6G) (Fig. S6).

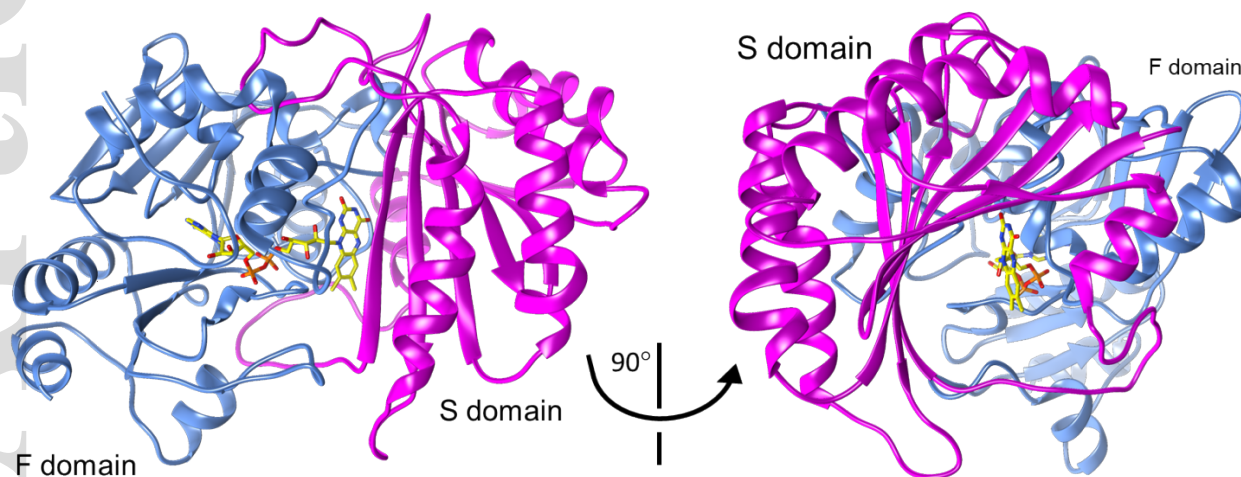


Fig. 3: Overall structure of ChitO from frontal and side view.

F and S domains are in blue and magenta, respectively. The FAD cofactor is in sticks with yellow carbon atoms.

The FAD cofactor is deeply embedded in the protein, except for the isoalloxazine ring. This redox active part of the flavin cofactor is exposed to the solvent because of its position at the bottom of a large opening. The isoalloxazine ring is covalently attached to the protein scaffold via a histidyl linkage to His64 and a cysteinyl linkage to Cys154 (Fig. 4), similar to GOO [14] (the corresponding residues are His70 and Cys130 in GOO). Other residues interacting with FAD, but not forming covalent bonds, are: 1) Tyr53, Tyr96, Thr153, Val157, His162, Tyr444 and Tyr447 with the isoalloxazine ring, 2) Asn446 with the ribityl moiety, 3) the backbone of Gly92 and Gly161 with the diphosphate moiety and 4) Ser91, His165 and Asn484 with the adenine. In our ligand-free structure, as mentioned above, the isoalloxazine ring of the FAD is quite exposed to the solvent. The crevice between the F and S domains allows positioning of saccharides of various length.

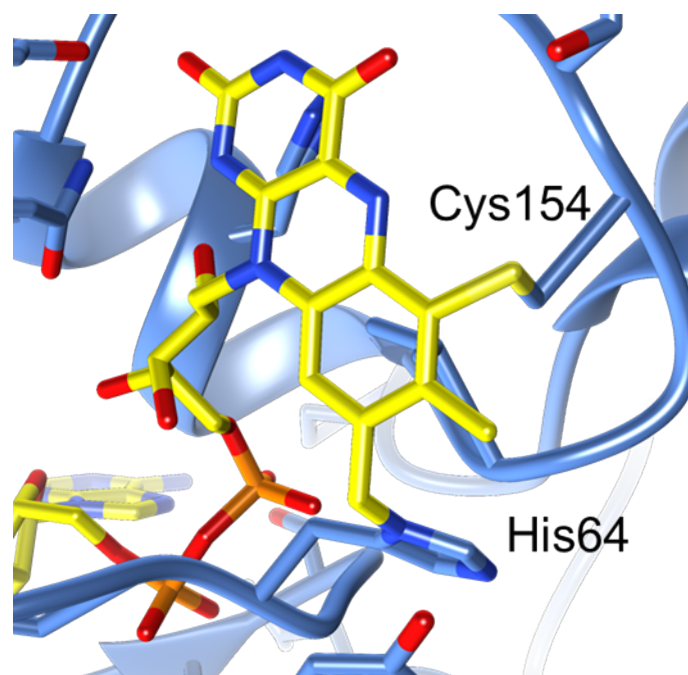


Fig. 4: The isoalloxazine ring of the FAD cofactor which is bicovalently bound to His64 and Cys154.

To have a better view on how substrates bind in the active site, *in silico* docking experiments have been performed. The results are in agreement with the substrate acceptance profile determined for ChitO. The analysed substrates are from two classes: (1) the above-mentioned N-glucosamine derivatives, and (2) several oligosaccharides. When the N-glucosamines were docked as ligands, they bound in the active site of ChitO by adopting a pro-catalytic arrangement (Fig. 5). Specifically, the CH-OH bond at position C1 points to a specific tyrosine residue (Tyr447) which can act as base (Fig. S7), while the C1 hydrogen points towards the isoalloxazine ring to undergo hydride transfer to the N5 of the FAD. The conservation of this tyrosine residue and of the isoalloxazine tethering shows that the basal catalytic machinery in ChitO, GOO and XyIO is conserved. In this conformation, the moiety at C2 is hosted in a secondary pocket consisting of residues Thr153, Tyr168, Met170, Gln268, Phe319, Gln375, Asn377, Tyr444 and Tyr447. This is perfectly in line with the reported finding that Gln268 is crucial for recognition of the N-acetyl moiety [21]. This pocket is located on one side of the isoalloxazine ring, and endows ChitO specificity towards N-acetylated compounds. In fact, the pocket that allows hosting groups bound to C2 was found to be quite large and suited for binding a C2-linked hydrophobic tail of considerable length. Docking of GlcVal, with a C2 alkyl moiety of 4 carbon atoms, was found to fit the secondary pocket, enclosed between Met170 and Phe319, and taking advantage of the

orientation of Tyr168, pointing away from the ligand. Docking of streptozotocin, which results in positioning of the nitrosourea in the same secondary pocket, suggests that the reduced affinity for this substrate with respect to GlcVal can be explained by the lack of favourable interactions available for the polar nitrosourea moiety. Met170, Phe319 and the methyl group of Thr153 surround this part of the docked streptozotocin structure. Initially, docking of the best reported substrate, GlcHex, did not result in a catalytically competent binding mode. Yet, when the side chains of Thr153, Met170 and Phe319 were allowed to rotate, a similar pose for the D-glucose moiety was obtained, while the aliphatic alkyl chain snugly fits in the secondary pocket (Fig. S8).

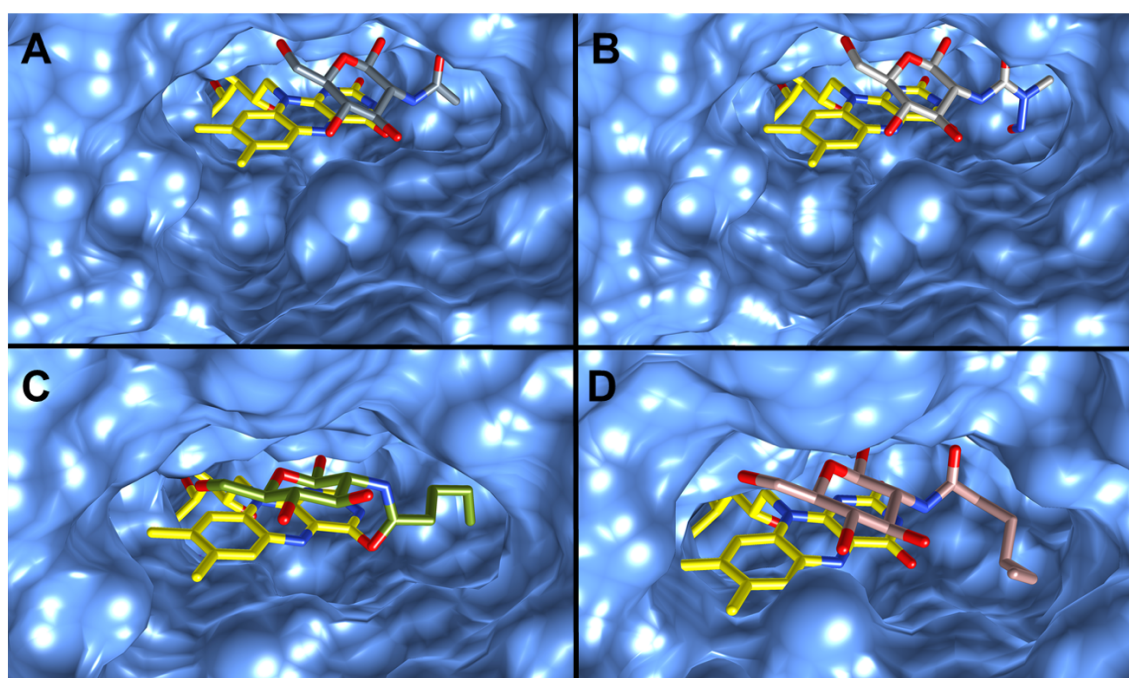


Fig. 5: Docked structures of N-acetylated compounds in the binding pocket of ChitO, represented as light blue surface. FAD is represented as yellow carbon atoms. Standard coding with red oxygen atoms and blue nitrogen atoms is retained for all stick representations. GlcNAc in grey carbon atoms (A), streptozotocin in white carbon atoms (B), GlcVal in dark green carbon atoms (C) and GlcHex in light pink carbon atoms (D) all bound in the reactive conformation with reducing end pointing the active site of the enzyme. The N-acetyl group retains the same binding mode.

These experiments confirm that such bulky aliphatic moieties can be accommodated in the secondary pocket. To explore whether ChitO would be able to bind substrates with a larger moiety at C2, we performed docking experiments using N-octanoyl-D-glucosamine (GlcOct). For this bulky substrate, like for GlcHex, flexibility of Thr153, Met170 and Phe319 was included in the

docking procedure. Despite multiple docking attempts, no binding pose was found that would be compatible with catalysis (Fig. S9). Even when allowing all residues that form the secondary pocket to move freely, no relevant binding was found which indicates that the long alkyl tail in GlcOct cannot be accommodated in the secondary pocket of ChitO. Unfortunately, GlcOct or a closely related glucosamine derivative is not commercially available, preventing experimental testing. The kinetic data, structural analysis together with the docking experiment have revealed a secondary largely hydrophobic pocket in ChitO in which residues Met170 and Phe319 play a pivotal structural role. In other reported sequence-related carbohydrate oxidases, these residues are typically replaced by Phe and Tyr residues, respectively (Fig. S6). The finding that ChitO harbours a pocket that allows binding of bulky moieties at the C2 position of D-glucose is intriguing and may suggest a role of ChitO in the modification of oligosaccharide different from chitooligosaccharides. While this is relevant to possible biotechnological applications, the role of this pocket still is enigmatic. Except for suggesting other substrates than chitin-derived compounds, the pocket may also serve another role such as an entry point or reservoir of dioxygen which also is hydrophobic [36].

We also performed docking with oligosaccharides as ChitO exhibits higher affinities towards chito-oligosaccharides when compared with the chitomonosaccharide N-acetylglucosamine, with the lowest K_m values observed for chitotriose and chitotetraose. Docking of chitobiose and chitotriose revealed that binding of such oligosaccharides does not interfere with the positioning of the reducing end, which is bound as observed for the above-mentioned monosaccharides (Fig. 6).

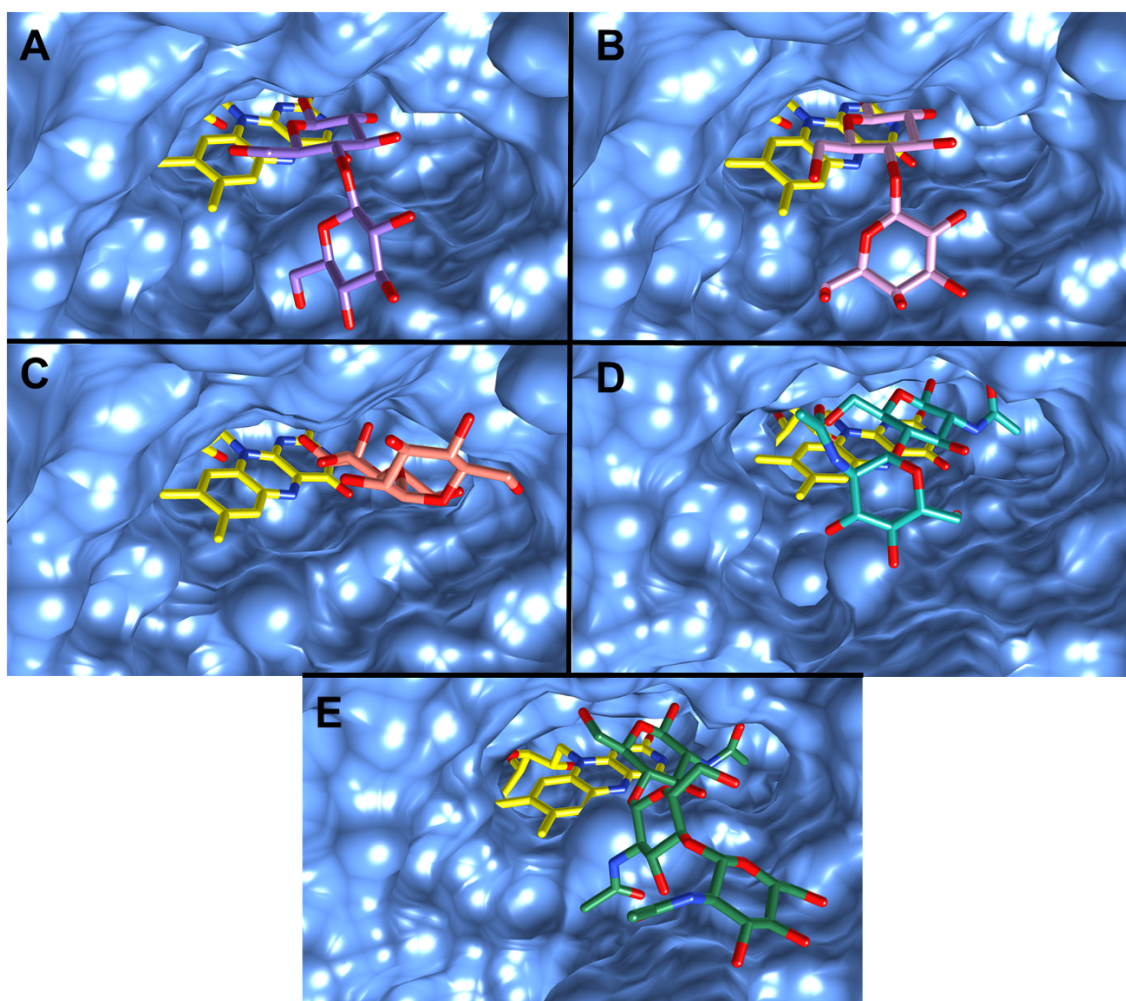


Fig. 6: Docked structures of disaccharides in the binding pocket of ChitO, represented as blue surface. FAD is represented as yellow carbon atoms. Standard coding with red oxygen atoms and blue nitrogen atoms is retained for all stick representations. Cellobiose in purple carbon atoms (A), lactose in pink carbon atoms (B) and maltose in salmon carbon atoms (C) all bound in the reactive conformation with the reducing end pointing the enzyme active site. In panels D and E are represented chitobiose and chitotriose, in cyan and green carbon atoms, respectively.

Docking shows that the oligosaccharides can bind in the extremely large funnel-like pocket that ChitO hosts, offering interactions with the side chain of the residues that shape the funnel, providing partial protection from the solvent. Other disaccharides docked in the ChitO crystal structure were cellobiose, lactose and maltose (Fig. 6 panels A-C). These sugars were chosen as they were reported as poor substrates of ChitO mainly due to high K_m values (> 50 mM) [21]. In order to retain the same catalytic arrangement displayed for previously docked sugars, because of its stereochemistry, maltose adopted a different binding mode, which is allowed by the large space

available in the binding pocket. On the contrary, the reducing ends of cellobiose and lactose bound similarly as found for GlcNAc. The poor binding of these substrates can be explained by the absence of a modification at C2, limiting the number of substrate-protein interactions.

In conclusion, our data reveal the structural basis for the unique substrate acceptance profile of ChitO from *Fusarium graminearum*. The bicovalent flavoprotein oxidase was found to act on a wider range of D-glucose derivatives. This includes a relaxed acceptance for modifications at C2, while it can bind and oxidise mono- and oligosaccharides. The novel findings shed a new light on the catalytic potential of ChitO, which may help in elucidating its physiological role. The data also can facilitate future engineering efforts with the aim of tailoring ChitO towards defined carbohydrates.

References

1. van Hellemond EW, Leferink NG, Heuts DP, Fraaije MW and van Berkel WJ (2006) Occurrence and biocatalytic potential of carbohydrate oxidases. *Adv Appl Microbiol.* **60**:17-54.
2. Salaheddin C, Takakura Y, Tsunashima M, Stranzinger B, Spadiut O, Yamabhai M, Peterbauer CK, Haltrich D (2010) Characterisation of recombinant pyranose oxidase from the cultivated mycorrhizal basidiomycete *Lyophyllum shimeji* (Hon-Shimeji). *Microb Cell Fact.* **9**:57.
3. M A McGuirl MA and Dooley DM (1999) Copper-containing oxidases. *Curr Opin Chem Biol.* **3** (2), 138-44.
4. Angel T Martínez *et al.* (2017) Oxidoreductases on their way to industrial biotransformations. *Biotechnol Adv.* **35** (6), 815-831.
5. Hecht HJ, Kalisz HM, Hendle J, Schmid RD and Schomburg D (1993) Crystal structure of glucose oxidase from *Aspergillus niger* refined at 2.3 Å resolution. *J Mol Biol.* **229** (1), 153-72.
6. Sützl L, Foley G, Gillam EMJ, Bodén M and Haltrich D (2019) The GMC superfamily of oxidoreductases revisited: analysis and evolution of fungal GMC oxidoreductases. *Biotechnol Biofuels* **12**, 118.
7. Wongnate T and Chaiyen P (2013) The substrate oxidation mechanism of pyranose 2-oxidase and other related enzymes in the glucose-methanol-choline superfamily. *FEBS J.* **280** (13), 3009-27.
8. Hallberg BM, Leitner C, Haltrich D and Divne C (2004) Crystal structure of the 270 kDa homotetrameric lignin-degrading enzyme pyranose 2-oxidase. *J Mol Biol.* **341**, 781–796.

9. Fraaije MW, van den Heuvel RHH, van Berkel WJH and Mattevi A (1999) Covalent flavinylation is essential for effective catalysis in vanillyl-alcohol oxidase. *The Journal of Biochemistry* **274** (50) 35514-35520.
10. Fraaije MW, van Berkel WJH, Benen JA, Visser J and Mattevi A (1998) A novel oxidoreductase family sharing a conserved FAD-binding domain. *Trends Biochem. Sci.* **23**, 206–207.
11. Leferink NGH, Heuts DPHM, Fraaije MW and van Berkel WJH (2008) The growing VAO flavoprotein family. *Archives of Biochemistry and Biophysics* **474**, 292-301.
12. Heuts DP, Scrutton NS, McIntire WS and Fraaije MW (2009) What's in a covalent bond? On the role and formation of covalently bound flavin cofactors. *FEBS J.* **276** (13):3405-27.
13. Lin SF, Yang TY, Inukai T, Yamasaki M and Tsai YC (1991) Purification and characterization of a novel glucooligosaccharide oxidase from *Acremonium strictum* T1. *Biochim Biophys Acta.* **1118** (1):41-7.
14. Huang CH, Lai WL, Lee MH, Chen CJ, Vasella A, Tsai YC and Liaw SH (2005) Crystal structure of glucooligosaccharide oxidase from *Acremonium strictum*: a novel flavinylation of 6-S-cysteinyl, 8 α -N1-histidyl FAD. *J Biol Chem.* **280** (46):38831-8.
15. Vuong TV, Vesterinen AH, Foumani M, Juvonen M, Seppälä J, Tenkanen M, Master ER (2013) Xylo- and cello-oligosaccharide oxidation by gluco-oligosaccharide oxidase from *Sarocladium strictum* and variants with reduced substrate inhibition. *Biotechnol Biofuels.* **6** (1):148.
16. Vuong TV, Master ER (2014) Fusion of a xylan-binding module to gluco-oligosaccharide oxidase increases activity and promotes stable immobilization. *PLoS One.* **9** (4):e95170.
17. Mewies M, McIntire WS and Scrutton NS (1998) Covalent attachment of flavin adenine dinucleotide (FAD) and flavin mononucleotide (FMN) to enzymes: the current state of affairs. *Protein Sci.* **7** (1):7-20.
18. Xu F, Golightly EJ, Fuglsang CC, Schneider P, Duke KR, Lam L, Christensen S, Brown KM, Jørgensen CT and Brown SH. (2001) A novel carbohydrate: acceptor oxidoreductase from *Microdochium nivale*. *Eur J Biochem.* **268** (4):1136-42.
19. Forneris F , Heuts DPHM, Delvecchio M, Rovida S, Fraaije MW and Mattevi A. (2008) Structural analysis of the catalytic mechanism and stereoselectivity in *Streptomyces coelicolor* alditol oxidase. *Biochemistry.* **47** (3), 978-85.

20. Ferrari AR, Rozeboom HJ, Dobruchowska JM, van Leeuwen SS, Vugts ASC, Koetsier MJ, Visser J and Fraaije MW. (2016) Discovery of a xylooligosaccharide oxidase from *Myceliophthora thermophila* C1. *J Biol Chem.* **291** (45), 23709-23718.
21. Liaqat F and Eltem R (2018) Chitooligosaccharides and their biological activities: A comprehensive review. *Carbohydr Polym.* **184** :243-259.
22. Heuts DPHM, Janssen DB and Fraaije MW (2007) Changing the substrate specificity of a chitooligosaccharide oxidase from *Fusarium graminearum* by model-inspired site-directed mutagenesis. *FEBS Lett.* **581**, 4905-4909.
23. Heuts DP, Winter RT, Damsma GE, Janssen DB and Fraaije MW (2008) The role of double covalent flavin binding in chito-oligosaccharide oxidase from *Fusarium graminearum*. *Biochem J.* **413**(1):175-83.
24. Ferrari AR, Lee M and Fraaije MW (2015) Expanding the substrate scope of chitooligosaccharide oxidase from *Fusarium graminearum* by structure-inspired mutagenesis. *Biotechnol Bioeng.* **112** (6):1074-80.
25. Ferrari AR, Gaber Y and Fraaije MW (2014) A fast, sensitive and easy colorimetric assay for chitinase and cellulase activity detection. *Biotechnol Biofuels* **10** ;7(1):37.
26. Foneris F, Orru R, Bonivento D, Chiarelli LR and Mattevi A (2009) ThermoFAD, a ThermoFluor®-adapted flavin ad hoc detection system for protein folding and ligand binding. *The FEBS Journal* **275** (10),2833-2840.
27. Kabsch W (2010) XDS. *Acta Crystallogr D Biol Crystallogr.* **66** (Pt 2):125-32.
28. Winn MD, Ballard CC, Cowtan KD, Dodson EJ, Emsley P, Evans PR, Keegan RM, Krissinel EB, Leslie AG, McCoy A, McNicholas SJ, Murshudov GN, Pannu NS, Potterton EA, Powell HR, Read RJ, Vagin A and Wilson KS (2011) Overview of the CCP4 suite and current developments. *Acta Crystallogr. D Biol. Crystallogr.* **67**, 235-242.
29. McCoy AJ, Grosse-Kunstleve RW, Adams PD, Winn MD, Storoni LC and Read RJ (2007) Phaser crystallographic software. *J. Appl. Crystallogr.* **40**, 658-674.
30. Emsley P and Cowtan K (2004) Coot: Model-building tools for molecular graphics. *Acta Crystallogr. D Biol. Crystallogr.* **60**, 2126-2132.
31. Krieger E and Vriend G (2002) Models@Home: distributed computing in bioinformatics using a screensaver based approach. *Bioinformatics.* **18** (2): 315–8.

32. Trott O and Olson AJ (2010) AutoDock Vina: improving the speed and accuracy of docking with a new scoring function, efficient optimization and multithreading. *Journal of Computational Chemistry* **31** (2010) 455-461.
33. <https://proteins.plus/help/protoss>
34. The PyMOL Molecular Graphics System, Version 2.0 Schrödinger, LLC.
35. Szkudelski T (2001) The mechanism of alloxan and streptozotocin action in B cells of the rat pancreas. *Physiol Res.* ;**50** (6):537–546.
36. Baron R, Riley C, Chenprakhon P, Thotsaporn K, Winter RT, Alfieri A, Forneris F, van Berkel WJH, Chaiyen P, Fraaije MW, Mattevi A, McCammon JA. (2009) Multiple pathways guide oxygen diffusion into flavoenzyme active sites. *Proc Natl Acad Sci* **106** (26): 10603–10608.